Cent. Eur. J. Phys. • 11(7) • 2013 • 894-903
DOI: 10.2478/s11534-013-0273-6

VERSITA

Central European Journal of **Physics**

Quench dynamics in spin crossover induced by high pressure

Research Article

Alexander I. Nesterov[1*], Sergey G. Ovchinnikov[2,3†], Grigorii A. Iaroshenko[1,2‡]

1 *CUCEI, Universidad de Guadalajara, Av. Revolución 1500, Guadalajara, 44420 Guadalajara, México*

2 *L. V. Kirensky Institute of Physics, SB RAS, Akademgorodok, 660036, Krasnoyarsk, Russia*

3 *Institute of Engeniering Physics and Radioelectronics, Siberian Federal University, Svobodny Prospect 79 , 660041, Krasnoyarsk, Russia*

Received 04 April 2013; accepted 22 June 2013

Abstract: In this paper we have analytically and numerically studied the dynamics of spin crossover induced by time-dependent pressure. We show that quasi static pressure, with a slow dependence on time, yields a spin crossover leading to transition from the high spin (HS) quantum system state to the low spin (LS) state. However, quench dynamics under shockwave load are more complicated. The final state of the system depends on the amplitude and pulse velocity, resulting in the mixture of the HS and LS states.

PACS (2008): 75.30.Wx, 03.65.-w, 03.65.Vf

Keywords: energy level crossing • spin crossover • quantum phase transition

1. Introduction

Spin crossover in condensed matter physics is the transformation of a system with a given spin S_1 at each lattice site into another state with spin S_2, induced by some external field, such as a strong magnetic field, high pressure, etc. It is accompanied by energy levels E_1 and E_2crossing, where E_a is the local energy of the magnetic ion with spin S_a $(a = 1, 2)$. Recently spin crossovers in magnetic oxides have been found under high pressure in $FeBO_3$ [1], $CdFe_3(BO_3)_4$ [2], $BiFeO_3$ [3] and Fe_3O_4 [4]. Below the Curie temperature, spin crossover is accompanied by a sharp change in the magnetization; nevertheless it may be observed in the paramagnetic state (e.g. in $CdFe_3(BO_3)_4$ [2]) as the sharp change of the XES satellite/main peak intensity ratio with increasing pressure.

Energy levels crossing results in the loss of analyticity in the energy spectrum at the critical point (in the thermodynamic limit) [5]. Near the critical point, adiabaticity breaks down and non-equilibrium phenomena associated with dramtically amplified quantum fluctuations can drive the system away from the ground state. The final result depends on how fast the transition occurs. If the quench

*E-mail: nesterov@cencar.udg.mx (Corresponding author)
†E-mail: sgo@iph.krasn.ru
‡E-mail: gri2086@mail.ru

process is sufficiently fast, large numbers of topological defects are created and the final state, being characterized by mixture of high and low spin phases, can be essentially different from that obtained as result of slow evolution. Qualitatively, quench dynamics can be described by the Kibble-Zurek theory of nonequilibrium phase transitions [6–8].

In this paper we consider quench dynamics in spin crossover induced by time-dependent pressure. The paper is organized as follows. In Sec. II, a general model of spin crossover under high pressure is introduced. In Sec. III, we study quench dynamics. We consider two cases: a) pressure defined as a linear function of time; b) pressure defined by a pulse of a given shape. We conclude in Sec. IV with a discussion of our results.

2. Model

The multielectron ion in a crystal field has the energies of terms for d^n configurations determined numerically by the Tanabe-Sugano diagrams [9] as a solution of the eigenvalue problem. Simple analytical calculations of the low energy terms with different spin values have recently been made [10], and these calculations were sufficient to study spin crossover. The crystal field parameter increases linearly with pressure P, thus the multielectron energies for spin S_1 and S_2 (E_1 and E_2) are also linear functions of P. To distinguish two different spin states in the lattice we introduce the Ising pseudospin states $|i\rangle$ and $|-i\rangle$ for $|d_i^n, S_1^i\rangle$ and $|d_i^n, S_2^i\rangle$, where i runs over all sites in the lattice. Thus we neglect the spin degeneracy of the d_i^n terms but capture the possibility of energy level crossing that is the essential part of the spin crossover. Then, in the basis $|i\rangle$, $|-i\rangle$, the Hamiltonian of the system can be written as follows

$$H = \sum_i \left(\lambda_0^i \mathbb{1} + \varepsilon_i \hat{\sigma}_i^z\right) + \sum_{ij} H_{ij}, \qquad (1)$$

where $\lambda_0^i = (E_1^i + E_2^i)/2$, $\varepsilon_i = (E_1^i - E_2^i)/2$, and $\mathbb{1}$, $\hat{\sigma}_z$ are the identity and Pauli matrices, respectively; the Hamiltonian of interaction between the spins being H_{ij}.

H_{ij} includes the isotropic Heisenberg term with the exchange interaction I_{ij} between nearest spins and the anisotropic term H_A. The interatomic interaction I_{ij} is negligibly small in comparison with the interatomic Hund's coupling (ratio 10^{-2}). Thus its contribution to the localized spin energy E_1 and E_2 due to the effective molecular field can be neglected. Nevertheless the exchange interaction plays very important role: it results in the long range order and synchronization of each spin in the same quantum state providing a cooperative behavior in the spin system. If it were the ferromagnetic interaction, each spin at T=0 would have the maximal projection S with integer magnetic moment $2S$.

In all examples given above there is the antiferromagnetic interaction. The ground state of the isotropic Heisenberg antiferromagnet has non-integer local magnetic moment due to the quantum spin fluctuations. It is known that for large spin S, the effect of quantum fluctuations is less important than for small spin, and for $FeBO_3$ the spin is 5/2. Moreover, the magnetic anisotropy suppresses quantum fluctuations. For example, in $FeBO_3$ the anisotropy field is $0.3T$ [11] and the measured value of the effective moment $2\sqrt{S(S+1)} = 5.9$ is very close to the calculated value of 5.916 for $S = 5/2$.

Thus we conclude that due to anisotropy the magnetic moment at $T = 0$ has integer value (of course it is a property of the magnetic insulator that does not hold for itinerant magnets), and due to the exchange interaction all spins are in the same quantum state. So spin crossover at $T = 0$ is the transition of the whole crystal from one magnetically ordered state to another. Nevertheless the criterion of the transition can be found from consideration of the single ion energy crossover due to space-uniform cooperative magnetic order. Anisotropic relativistic interactions, for example a spin-orbital interaction, are also important because they can mix different spin states inside a single ion.

We consider spin crossover far from the thermodynamic phase transition in the paramagnetic phase, allowing us to simplify this interaction and substitute the effect of exchange with the effective mean field. This mean field is spatially uniform for the ferromagnetic insulator or two-sublattice in the antiferromagnetic case. Examples given above [1–4] correspond to the anti- or ferromagnetics. In any case this mean field simply renormalizes the interionic multielectron energies E_1 and E_2, and is irrelevant to the crossover phenomenon. Another interaction that is smaller than the exchange interaction is given by relativistic anisotropy contribution to H_{ij}. For example a spin-orbital interaction can mix different spin states inside single ion, and it is found to be important in our problem.

In what follows we will consider the simplified spatially uniform model [12]. Motivation for this simplification is as follows. Although spin crossover is related to a many body system, the essential features of its dynamics can be described by a Landau-Zener type effective Hamiltonian [13].

The Hamiltonian of our model is given by $\mathcal{H} = \sum_{i=1}^{N} \mathcal{H}_i$, where

$$\mathcal{H}_i = \begin{pmatrix} \lambda_0 & 0 \\ 0 & \lambda_0 \end{pmatrix} + \begin{pmatrix} \varepsilon & \rho e^{-i\varphi} \\ \rho e^{i\varphi} & -\varepsilon \end{pmatrix}. \qquad (2)$$

The energy spectrum is given by $\varepsilon_{\pm} = \lambda_0 \pm \sqrt{\varepsilon^2 + \rho^2}$. Both λ_0 and ε are pressure dependent. Further we assume that the spin excitation gap is given by

$$\varepsilon(P) = \varepsilon_0 \left(1 - \frac{P}{P_c}\right). \tag{3}$$

The crossover takes place at the point P_c, where $\varepsilon(P_c) = 0$. The spin-orbit coupling $\lambda = \rho e^{i\varphi}$ (with $\rho \ll \varepsilon_0$) mixes the different spin states, and plays the role of quantum fluctuations in our Ising pseudospin basis. The dimensionless spin gap, $P/P_c - 1$, plays the role of relative temperature ($T/T_c - 1$) near the critical point T_c [14].

3. Quench dynamics induced by high pressure

We consider time dependent Schrödinger equation for the Hamiltonian (2) assuming for simplicity that the pressure is a linear function of time, $P = P_c(1 + t/\tau_Q)$. Inserting this expression into Eq. (3), we obtain $\varepsilon(t) = -\varepsilon_0 t/\tau_Q$. The parameter τ_Q depends on $\dot{P}$ and can be written as $\tau_Q = P_c/\dot{P}$.

Let $|1\rangle$ and $|0\rangle$ be eigenstates of the operator $\hat{\sigma}_z$, so that $\hat{\sigma}_z|1\rangle = |1\rangle$ and $\hat{\sigma}_z|0\rangle = -|0\rangle$. Expressing a generic state vector as

$$|\psi(t)\rangle = e^{-i\int \lambda_0(t)dt}(C_1(t)e^{-i\varphi/2}|1\rangle + C_0(t)e^{i\varphi/2}|0\rangle), \tag{4}$$

we find that the coefficients $C_1(t)$ and $C_0(t)$ satisfy the Schrödinger equation with the time-dependent Hamiltonian in the Landau-Zener (LZ) form (in units $\hbar = 1$)

$$i\frac{d}{dt}\begin{pmatrix} C_1(t) \\ C_0(t) \end{pmatrix} = \begin{pmatrix} -\Delta t & \rho \\ \rho & \Delta t \end{pmatrix}\begin{pmatrix} C_1(t) \\ C_0(t) \end{pmatrix}, \tag{5}$$

where $\Delta = \varepsilon_0/\tau_Q$.

In terms of dimensionless scaled time $\tau = \sqrt{\Delta}t = \tau_0(P/P_c - 1)$ with $\tau_0 = \sqrt{\varepsilon_0\tau_Q} = \sqrt{\varepsilon_0 P_c/\dot{P}}$, the Landau-Zener model is described by the Hamiltonian

$$\mathcal{H} = \begin{pmatrix} -\tau & \omega \\ \omega & \tau \end{pmatrix}, \tag{6}$$

where $\omega = \rho/\sqrt{\Delta} = \tau_0\rho/\varepsilon_0$ is the dimensionless coupling constant. Writing $|u(\tau)\rangle = C_1(\tau)|1\rangle + C_0(\tau)|0\rangle$, one can recast the Schrödinger equation (5) as

$$i\frac{d}{d\tau}|u(\tau)\rangle = \mathcal{H}(\tau)|u(\tau)\rangle. \tag{7}$$

Here the time τ runs from the initial time $\tau_i = -\sqrt{\varepsilon_0\tau_Q}$, corresponding to the initial pressure $P_i = 0$, to final $\tau_f = (P_f/P_c - 1)\sqrt{\varepsilon_0\tau_Q}$, corresponding to P_f at the end of quench ($P_f > P_c$). Further we assume that $\varepsilon_0\tau_Q \gg 1$; then time τ can be extended to $\pm\infty$, and the problem becomes fully equivalent to the LZ problem.

The energy spectrum of the Hamiltonian (6) is given by $\varepsilon_{\pm}(\tau) = \pm\sqrt{\tau^2 + \omega^2}$, and its instantaneous eigenvectors can be written as

$$|u_-(\tau)\rangle = \begin{pmatrix} -\sin\frac{\theta(\tau)}{2} \\ \cos\frac{\theta(\tau)}{2} \end{pmatrix}, \; |u_+(\tau)\rangle = \begin{pmatrix} \cos\frac{\theta(\tau)}{2} \\ \sin\frac{\theta(\tau)}{2} \end{pmatrix}, \tag{8}$$

where $\cos\theta(\tau) = -\tau/\sqrt{\tau^2 + \omega^2}$. The energy gap between the ground and excited states equals $2\sqrt{\tau^2 + \omega^2}$.

From Eq. (8) it follows that while the ground state behaves at $\tau = \pm\infty$ as $|u_-(-\infty)\rangle \to |0\rangle$ and $|u_-(+\infty)\rangle \to |1\rangle$, the excited state behaves as follows: $|u_+(-\infty)\rangle \to |1\rangle$ and $|u_+(+\infty)\rangle \to |0\rangle$. The state $|u_-(-\infty)\rangle$ corresponds to the high spin (HS) of the system and $|u_+(-\infty)\rangle$ corresponds to the low spin (LS). Thus, if the system initially was in the HS state, at the end of the evolution its ground state corresponds to the LS. Tunnelling between the positive and negative energy eigenstates, leading to the mixture of HS and LS, happens in the neighbourhood of the critical point $\tau_c = 0$ ($P = P_c$) when $\tau \in (-\omega, \omega)$ [15].

We assume further that the evolution of the system starts at the moment of time $\tau_i = -\sqrt{\varepsilon_0\tau_Q}$ ($P(\tau_i) = 0$) from the ground state $|u_-(\tau_i)\rangle$. Since $\rho \ll \varepsilon_0$, we have $|u_-(\tau_i)\rangle \propto |0\rangle$. This yields the following initial conditions: $C_0(\tau_i) = 1$ and $C_1(\tau_i) = 0$. At the end of evolution we obtain $|u_-(\tau) \to |1\rangle$, while $\tau \to +\infty$.

In Figs. 1 – 2 we present the results of a numerical solution of the Schrödinger equation. In Fig. 1 time evolution of the Bloch vector, $\mathbf{n} = \langle u|\boldsymbol{\sigma}|u\rangle$, is shown. The motion begins at the south pole of the two-dimensional sphere S^2 and for $\omega = 3$ ends at the north pole. However for the choice of the parameter $\omega < 1$, numerical simulation shows that the Bloch vector never reaches the north pole, which corresponds to the LS state. This implies that at the end of evolution the quantum system does not remain in the ground state and its final state is the mixture of the HS and LS states.

In Fig. 2 the probability $P_\tau = |C_1(\tau)|^2$ of transition $|0\rangle \to |1\rangle$ is depicted for various values of ω. As can be seen, with decreasing adiabadicity parameter ω , the transition probability decreases as well. Its asymptotic behaviour is described by the LZ formula (14).

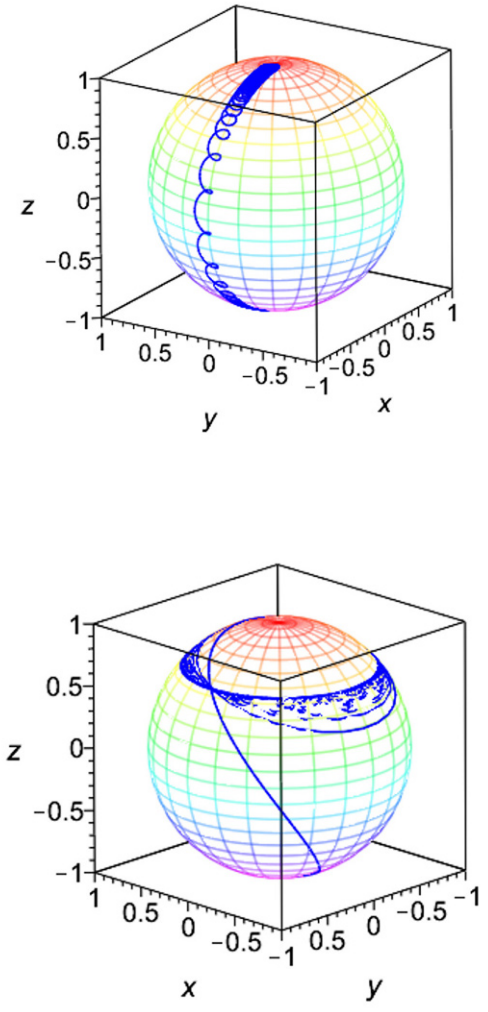

Figure 1. (Color online) Bloch vector's dynamics. The evolution starts at the south pole of the sphere. Top panel: ($\omega = 3$). Bottom panel: $\omega = 0.75$.

3.1. Exact solution of the Landau–Zener problem

The exact solution of Eq.(7) is given in terms of the parabolic cylinder functions [16–18], $D_{-1-i\omega^2/2}(z)$, where $z = \sqrt{2}\,\tau e^{-i\pi/4}$. Assuming that initially the system was in the ground state, $|u_-(-\infty)\rangle \to |0\rangle$, we obtain the initial conditions as follows: $C_0(-\infty) = 1$ and $C_1(-\infty) = 0$. The probability of transition to the state $|1\rangle$ at time τ is given

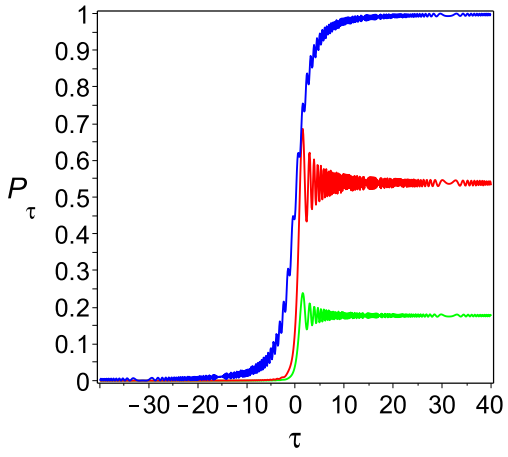

Figure 2. (Color online) Probability of transition P_τ obtained from exact solution of LZ problem as function of τ. From top to bottom: $\omega = 3, 0.5, 0.25$.

by [18–20]

$$P_\tau = \frac{\omega^2}{2} e^{-\pi\omega^2/4} \left| D_{-1-i\omega^2/2}(\tau\sqrt{2}e^{3i\pi/4}) \right|^2. \qquad (9)$$

As can be shown, the condition $\varepsilon_0 \gg \rho$ may be recast to $|\tau_i| \gg \omega$, where $\tau_i = -\sqrt{\varepsilon_0 \tau_Q}$ is the initial time. Since $|\tau_i| \gg 1$, for $\tau > |\tau_i|$ the so-called *weak-coupling asymptotic* approximation may be applied [18]. The asymptotic of the transition probability is

$$P_\tau \sim 1 - e^{-\pi\omega^2} - \frac{2\omega}{\tau} e^{-\pi\omega^2/2} \sqrt{1 - e^{-\pi\omega^2}} \cos\xi_w(\tau), \quad (10)$$

where

$$\cos\xi_w(\tau) = \frac{\pi}{4} + \tau^2 + \frac{\omega^2}{2}\tau^2 \ln 2 + \arg\Gamma\left(1 - i\frac{\omega^2}{2}\right). \quad (11)$$

3.1.1. Adiabatic approximation

The commonly used version of the adiabatic theorem takes the form [20–22]

$$\frac{\max |\langle \psi_e | dH_\tau(t)/dt | \psi_g \rangle|}{\min |E_e(t) - E_g(t)|^2} \ll 1, \qquad (12)$$

where $|\psi_g\rangle$ and $|\psi_e\rangle$ are the instantaneous ground state and the first excited state of the the total system.
For the LZ Hamiltonian (6), the condition for adiabatic evolution, required by the adiabatic theorem, is $\omega^2 \gg 1$

[19]. In the adiabatic approximation the probability of the system to remain in the ground state may be described by

$$P_{ad}(\tau) = |\langle u_-(\tau)|0\rangle|^2 = \frac{1}{2}\left(1 + \frac{\tau}{\sqrt{\tau^2+\omega^2}}\right). \qquad (13)$$

In Fig. 3 the probability of the adiabatic transition (red line) and the results of the exact solutions (blue line) are depicted. The figures show that for $\omega = 3$ there is a good agreement between the exact solution and the adiabatic formula (13), but that no such agreement is seen for $\omega = 0.5$. The probability of remaining in the ground state at the end of evolution ($\tau \to \infty$) is given by $P_{ad} = |C_1(+\infty)|^2$. For slow evolution we can use the LZ formula [23, 24] to describe the probability of adiabatic evolution:

$$P_{ad} = 1 - e^{-\pi\omega^2}. \qquad (14)$$

Using the so-called *adiabatic-impulse* (AI) approximation [13, 15], qualitatively, the dynamics of the Landau-Zener model can be described by the Kibble-Zurek theory of nonequilibrium phase transitions [6–8]. The AI-approximation assumes that the whole evolution can be divided in three parts and up to the phase factor the wave $|u(t)\rangle$ function can be approximated to:

$$\begin{aligned} \tau \in [-\infty, -\hat{\tau}]: &\quad |u(\tau)\rangle \approx |u_-(\tau)\rangle, \\ \tau \in [-\hat{\tau}, \hat{\tau}]: &\quad |u(\tau)\rangle \approx |u_-(-\hat{\tau})\rangle, \\ \tau \in [\hat{\tau}, +\infty]: &\quad |\langle u(\tau)|u_-(\tau)\rangle|^2 = \text{const}, \end{aligned}$$

where the time $\hat{\tau}$, introduced by Zurek [7], is called the *freeze-out time* and defines the instant when the behaviour of the system changes from the adiabatic regime to an impulse one where its state is effectively frozen and then back from the impulse regime to the adiabatic one.
If the evolution starts at moment $\tau_i \ll -\hat{\tau}$ from the ground state, the equation for determining $\hat{\tau}$ reads $\pi\hat{\tau}/2 = 1/\text{gap}(\hat{\tau})$ (for details of calculation see Ref. [13]), and its solution is given by

$$\hat{\tau} = \frac{\omega}{\sqrt{2}}\sqrt{\sqrt{1+\frac{4}{\pi^2\omega^4}} - 1}. \qquad (15)$$

Using the relation $\tau = \tau_0(P/P_c - 1)$, we find that the change of the adiabatic regime to a non-adiabatic one occurs when the pressure is $P_1 = P_c\left(1 - \hat{\tau}/\tau_0\right)$, and the non-adiabatic evolution becomes adiabatic again when the pressure increases to $P_2 = P_c\left(1 + \hat{\tau}/\tau_0\right)$. From here we find that within the pressure interval $\Delta\hat{P} = P_2 - P_1 = 2P_c\hat{\tau}/\tau_0$, the behaviour of the system is described by the impulse regime. Employing Eq. (15), we approximate $\Delta\hat{P}$ for fast ($\omega^2 \ll 1$) and slow ($\omega^2 \gg 1$) transitions as

$$\frac{\Delta\hat{P}}{P_c} = \begin{cases} \dfrac{1}{\sqrt{\pi}\tau_0}, & \omega^2 \ll 1 \\ \dfrac{1}{\pi\omega\tau_0}, & \omega^2 \gg 1. \end{cases} \qquad (16)$$

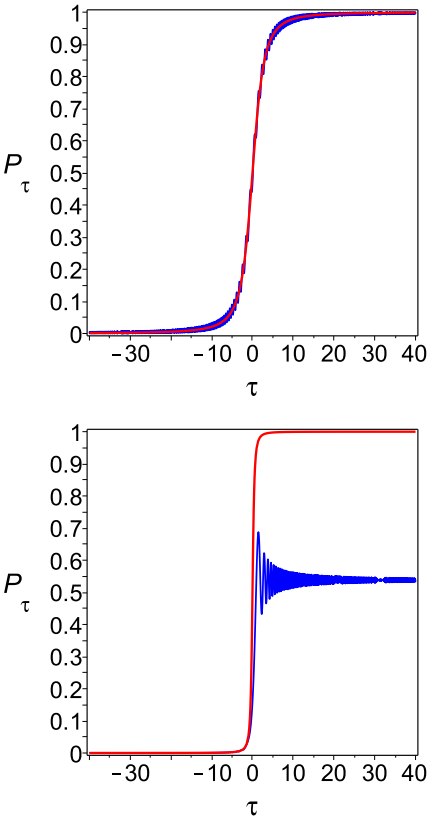

Figure 3. (Color online) Probability of transition $|0\rangle \to |1\rangle$ as function of dimensionless time τ. Top panel: red line: probability of adiabatic transition, $P_{ad}(\tau)$; blue line: probability of transition P_τ obtained from the exact solution of the LZ problem ($\omega = 3$). Bottom panel: red (upper) line: probability of adiabatic transition; blue (lower) line: transition probability obtained from exact solution of the LZ problem ($\omega = 0.5$).

In the AI approximation the probability, P_e, of finding the system in the excited state at $\tau_f \gg \hat{\tau}$ can be calculated as follows [13, 15]:

$$P_e \approx P_{AI} = |\langle u_+(\hat{\tau})|u_-(-\hat{\tau})\rangle|^2 = \frac{\hat{\tau}^2}{\omega^2+\hat{\tau}^2}. \qquad (17)$$

Substituting $\hat{\tau}$ from (15), we obtain

$$P_{AI} = \frac{2}{x^2 + x\sqrt{x^2+4}+2}, \qquad (18)$$

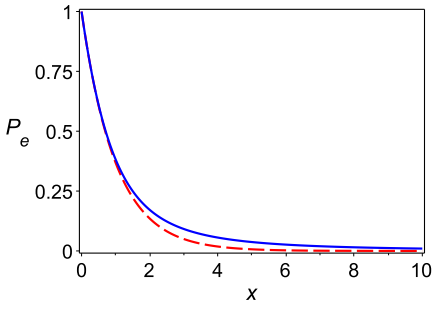

Figure 4. (Color online) Probability, P_e, of finding the system in the excited state ($x = \pi\omega^2$): blue line – $P_e \approx P_{AI}$ (17), dashed red line – the LZ expression, $P_e = e^{-\pi\omega^2}$.

where $x = \pi\omega^2$. For $\omega^2 \ll 1$, from Eq. (18) it follows that $P_{AI} \approx 1 - \pi\omega^2$. In the first order this coincides with the result predicted by the exact LZ formula: $P_e = e^{-\pi\omega^2}$. For the adiabatic evolution, $\omega^2 \gg 1$, we obtain $P_{AI} \approx 1/\pi^2\omega^4$ (see Fig. 4.). As can be seen, the AI approximation is good enough for $\omega^2 \leq 1$ and in the limit $\omega^2 \gg 1$.

Comparison with experimental data. – To compare our theoretical finding with the experiments on spin crossover under the high pressure we use the data from Refs. [1–4]. The typical value of the critical pressure in Fe oxides is $P_c = 50$ GPa, and the rest of parameters are taken as follows: $\varepsilon_0 = 1$ eV, $\rho = 0.01$ eV and $\tau_Q \approx 10^4$ s. The computation yields: $\tau_0 \approx 10^9$ and $\omega \approx 10^7$. Thus the spin crossover under slowly changed pressure realized in the cited experiments is a highly adiabatic process ($\omega^2 \gg 1$). Using (16), we find the that the domain of non-adiabaticity is defined by $\Delta\hat{P} \approx 10^{-7}$ Pa. The corresponding interval of time $\hat{t} \approx 1/(\pi\rho\tau_0)$ is $\hat{t} \approx 10^{-21}$ s. Thus we have obtained the evident conclusion that the non-adiabatic effect under static pressure is negligible. In the next section we demonstrate that for a dynamical loading the non-adiabatic effects may be rather strong.

3.2. Quench dynamics under shock-wave load

In this section we study the quench dynamics in the spin system under time-dependent pressure, $P(t)$. We assume that at the initial moment of time $P(t_i) = 0$. Further it is convenient to present $P(t)$ as $P(t) = P_0 s(t)$, where the function $s(t)$ determines the pulse shape. We assume that its maximum is $s_m = 1$.

One can observe that the first term in the Hamiltonian (2), yielding contribution to the total phase factor of the the wave function, does not affect the dynamics of the system and may be omitted. Setting for simplicity $\varphi = 0$ and using Eq. (3), one can recast the time-dependent driving Hamiltonian as follows:

$$\mathcal{H}_\tau(t) = \begin{pmatrix} \varepsilon_0(1 - as(t)) & \rho \\ \rho & -\varepsilon_0(1 - as(t)) \end{pmatrix}, \qquad (19)$$

where $a = P_0/P_c$. For a given a, the crossover occurs at the critical point $s_c = s(t_c)$ defined as $s_c = 1/a$.

Applying the adiabatic theorem, we find that condition for adiabatic evolution can be written as follows:

$$\left| \frac{dP(t)/dt}{\rho\sqrt{(1 - P(t)^2) + \beta^2}} \right| \ll 1, \qquad (20)$$

where $\beta = \rho/\varepsilon_0$. In what follows we study spin crossover for semi-infinite and finite pulse.

3.2.1. Semi-infinite pulse.

We specify the pressure as a semi-infinite pulse with the shape determined by

$$P = \begin{cases} 0, & t < 0 \\ P_0 \tanh(\alpha t), & t \geq 0, \end{cases} \qquad (21)$$

where P_0 is the pulse height.

For $P_0 = P_c$, expanding $P(t)$ near of the critical point up to the first order, we obtain the related LZ problem: $P(t) = P_c(1 + \alpha t)$. From here we obtain the corresponding LZ adiabaticity parameter as $\omega_{LZ} = \rho/\sqrt{\alpha\varepsilon_0}$. Next using Eq. (21), we obtain

$$\frac{1}{\omega_{LZ}^2} \max_{0<s<1} \left| \frac{a\beta(1 - s^2)}{\sqrt{(1 - as)^2 + \beta^2}} \right| \ll 1. \qquad (22)$$

In terms of the function $\omega(s)$ defined as

$$\frac{1}{\omega^2} = \frac{1}{\omega_{LZ}^2} \frac{a\beta(1 - s^2)}{\sqrt{(1 - as)^2 + \beta^2}}, \qquad (23)$$

the condition of adiabaticity (22) can be recast to the following:

$$\max_{0<s<1} \left(\frac{1}{\omega^2(s)} \right) \ll 1. \qquad (24)$$

In Fig. 5 (top panel) the function $1/\omega^2(s)$ is depicted for ω_{LZ} =1. We observe that $1/\omega^2$ has a maximum at the

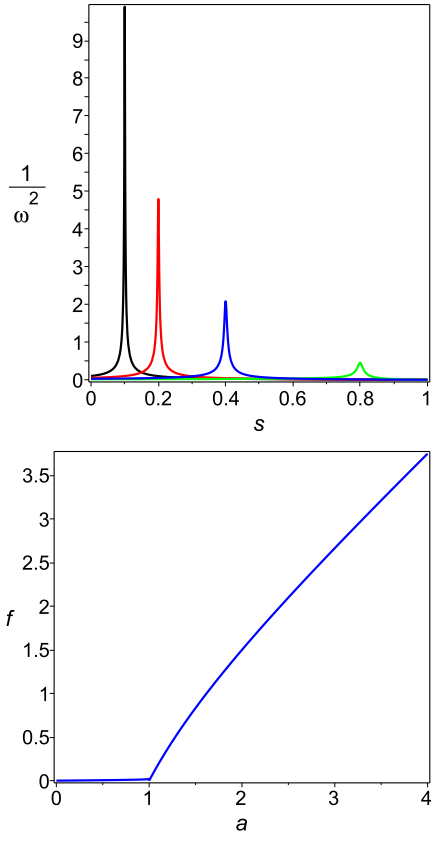

Figure 5. (Color online) Top panel. Parameter of adiabaticity as function of s. From the left to the right: $a = 10, 5, 2.5, 1.25$ ($\omega_{LZ} = 1$). Bottom panel. Dependence of the function $f(a)$ on the amplitude $a = P_0/P_c$ ($\beta = 0.01$).

critical point. This is in agreement with the general observation on the breakdown of adiabaticity in the neighbourhood of the critical point. For $\beta \ll 1$ we obtain the following estimate

$$\frac{1}{\omega^2} \approx \frac{f(a)}{\omega_{LZ}^2}, \tag{25}$$

where

$$f(a) = \begin{cases} \dfrac{2a\beta\sqrt{1-a^2}}{(1+\sqrt{1-a^2})\sqrt{1-a^2+\beta^2}}, & a \le 1 \\ a - 1/a, & a \ge 1 \end{cases} \tag{26}$$

In Fig. 5 (bottom panel) the function $f(a)$ is depicted. As can be observed $f(a) \approx 0$ for $a \le 1$.

In Figs. 6 - 7 we present the results of numerical calculations for different choices of parameter a. In all calculations the parameters were chosen as follows: $\varepsilon_0 = 1$ eV, $\rho = 0.01$ eV and $\alpha = 10\,\text{ns}^{-1}$. This yields $\omega_{LZ} = 1$, and for $\beta = \rho/\varepsilon_0$, we obtain $\beta = 0.01$. Fig. 6 (top panel) shows that for $P_0 = P_c$, independently of the initial conditions, the final state of the system is defined by the equal mixture of HS and LS states. The reason for this phenomena is in growing quantum fluctuations which lead to the mixture of HS and LS states at the critical pressure P_c. In Fig. 6 (bottom panel) the dependence of transition probability on time and pressure is depicted for different values of the dimensionless amplitude of the pulse, $a = P_0/P_c$. In the pressure interval $0 < P \lesssim 1.25P_c$, the evolution is highly adiabatic, and for $P_0 \approx 1.25P_c$ the system comes to the LS state with the minimal density of defects. However with the increasing of pressure amplitude, P_0, the probability of passing to the LS state decreases, and the system remains in the mixture of the HS ans LS states. Further increasing of the amplitude leads to the domination of the HS population over the LS population.

3.2.2. Finite pulse.

We consider a pressure pulse with a shape determined by $P = as(\tau)$, where $a = P_0/P_c$, $\tau = \alpha t$ is scaled dimensionless time, and

$$s(\tau) = \frac{\tanh(\tau - \delta) - \tanh(\tau - \delta - \Delta)]}{2\tanh\frac{\Delta}{2}}, \tag{27}$$

the pulse length being Δ (see Fig. 8). Applying the adiabatic theorem, we find that for the pulse (16), the condition for adiabatic evolution is given by $\max(1/\omega^2) \ll 1$, where

$$\frac{1}{\omega^2} = \left| \frac{\alpha a \left(\tanh^2(\tau-\delta) - \tanh^2(\tau-\delta-\Delta) \right)}{2\rho \tanh\frac{\Delta}{2}\sqrt{\left(1 - \frac{a(\tanh(\tau-\delta) - \tanh(\tau-\delta-\Delta))}{2\tanh\frac{\Delta}{2}}\right)^2 + \beta^2}} \right| \ll 1. \tag{28}$$

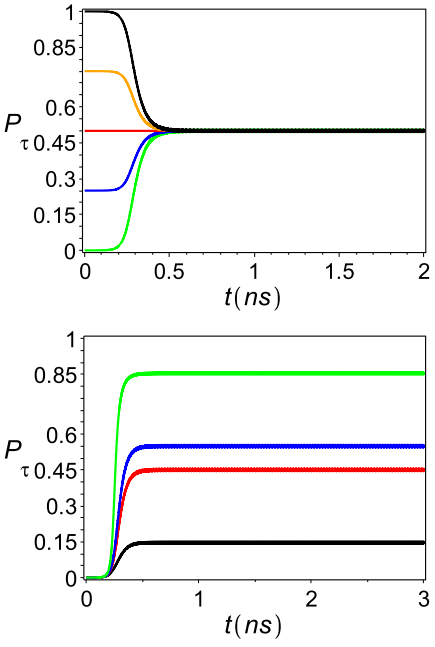

Figure 6. (Color online) Top panel. Dependence of transition probability P_τ on time t, for different initial conditions ($P_0 = P_c$). From up to down: $|C_0(0)|^2 = 0, 0.25, 0.5, 0.75, 1$ ($\alpha = 10\,\mathrm{ns}^{-1}$). Bottom panel. Transition probability P_τ for different values of the pulse height as function of time t. From up to down: $a = P_0/P_c = 1.01, 1.001, 0.999, 0.99$ ($\alpha = 10\,\mathrm{ns}^{-1}$).

The dependece of the function $1/\omega^2$ on dimensionless time τ and amplitude a is presented in Fig. 9. As we can see, the condition of adiabaticity is extremely sensitive to the choice of parameters $\kappa = \alpha/\rho$ and $a = P_0/P_c$. Violation of the adiabatic theorem may occur in the vicinity of the critical points, associated with the pulse boundaries. For $P_0 \gtrsim P_c$, one should impose the condition $\kappa \ll 1$ to satisfy the requirement of the adiabatic theorem.

Our theoretical predictions are confirmed by the results of numerical simulation presented In Fig. 10.

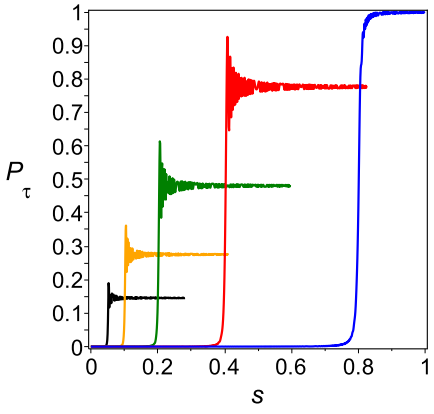

Figure 7. (Color online) Transition probability P_τ as function of scaled pressure s for different values of the pulse height ($\alpha = 10\,\mathrm{ns}^{-1}$). From the left to the right: $a = P_0/P_c = 20, 10, 5, 2.5, 1.25$.

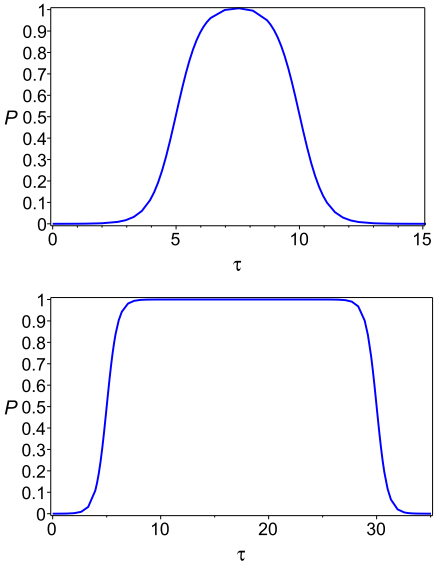

Figure 8. (Color online) Shape of finite pulse. Top panel: $\Delta = 5$. Bottom panel: $\Delta = 25$.

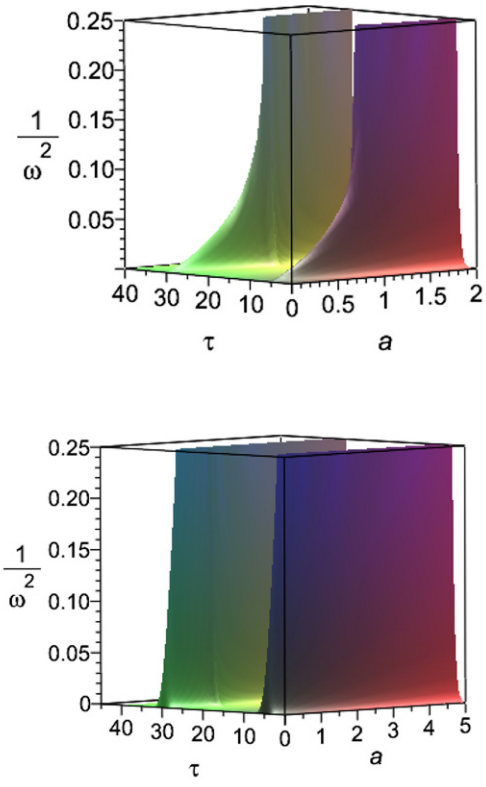

Figure 9. (Color online) Dependence of function $1/\omega^2$ on amplitude $a = P_0/P_c$ and τ. Top panel: $\alpha/\rho = 0.1$. Bottom panel: $\alpha/\rho = 1$ ($\Delta = 25$).

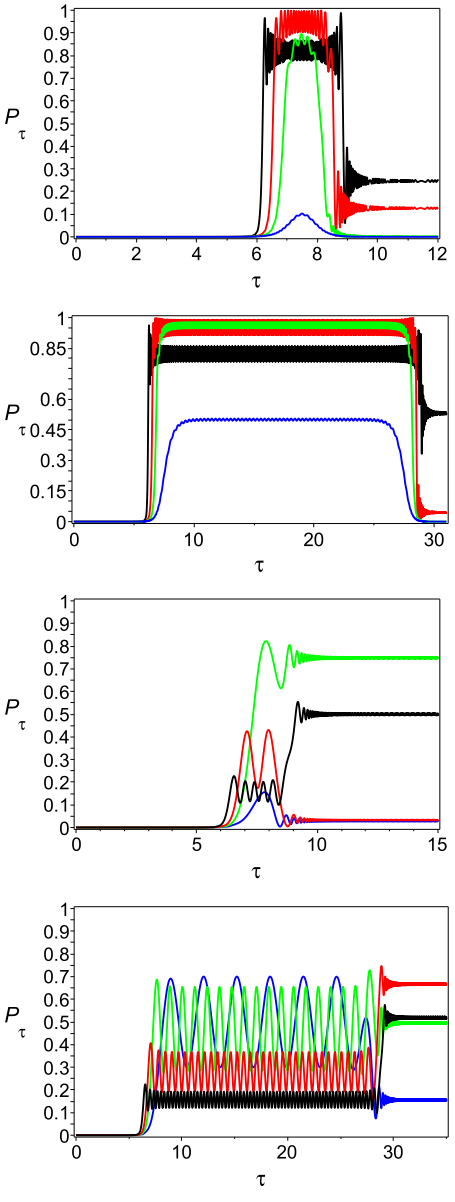

Figure 10. (Color online) Transition probability P_τ as function of time for different values of $a = P_0/P_c$ ($a = 1\,(blue), 1.025\,(green), 1.05\,(red), 1.1\,(black)$). First two panels from the top: $\Delta = 5$. Two panels from the bottom: $\Delta = 25$. First and third panel from the top: $\kappa = \alpha/\rho = 0.1$. Second and fourth panel: $\kappa = \alpha/\rho = 1$.

4. Conclusion

We have analytically studied the properties of spin crossover under high pressure. We showed that at static loading and $P = P_c$, occupation numbers of both HS and LS states are equal at zero temperature ($T = 0$), $n_{HS} = n_{LS} = 0.5$. For $P < P_c$ we obtain $n_{HS} = 1$ and $n_{LS} = 0$, while for $P > P_c$ one has $n_{HS} = 0$ and $n_{LS} = 1$. Static transition at $T = 0$ is a sharp quantum phase transition with a geometric Berry-like phase being the order parameter [12]. Finite temperature removes the singularity in the $n_{HS}(P)$ dependence. Thermal fluctuations between the two states $|0\rangle$ and $|1\rangle$ result in a smooth crossover instead of the quantum phase transition at $T = 0$.

To verify our theoretical predictions we have performed numerical simulations. Fig. 6 shows that the temporal quantum fluctuations have an effect similar to the thermal fluctuations. Small deviations from unity of the shock-wave amplitude P_0/P_c, result not in a sharp change of the probability P_τ either to zero or to unity but to a continuous deviation of the P_τ from the 0.5 value. At the same time for $P_0/P_c = 1$ any initial distribution of the HS and LS states will end its evolution in the equilibrium state $n_{HS} = n_{LS} = 0.5$ (Fig. 6). This conclusion is valid for any choice of parameter α.

Another dynamical effect worthy of discussion is that of the adiabaticity violations near the critical pressure (Fig. 7). This is a manifestation of the general Kibble-Zurek theory. The results shown in Fig. 7 are counter-intuitive at first glance. The shockwave with larger amplitude has smaller final probability for spin crossover and larger probability to stay in the initial HS state. To understand this effect one should note that the characteristic scale of the pressure increase is given by the factor $a\alpha$ for the wave with amplitude a. Thus a larger amplitude wave also is faster. Concerning experimental studies of the spin crossover under dynamical loading, it is clear from our results that for some parameters of the loading the final state will be a mixture of the HS and LS states, even if the maximal value of applied pressure was above the critical value. It is known from experiments that at dynamical loading the spin crossover may be spread over a wide pressure interval (about 100 GPa), while under static pressure with isotropic medium in the diamond anvil cell the crossover is very narrow [25].

Acknowledgments

This research was supported by the President of Russia Grant NSh-1044.2012.2, Presidium of the Russian Academy of Science Project 2.16, RFBR Grant 12–02-90410_a and Siberian Federal University Grant F-11, A.I. Nesterov acknowledges the support from the CONACyT, Grant No. 15439. Grigorii A Iaroshenko acknowledges the support from the CONACyT, Grant No. 449614.

References

[1] V. A. Sarkisyan, I. A. Trojan, I. S. Lyubutin et al., JETP Lett. 76, 426 (2002)
[2] A. G. Gavriliuk, S. A. Kharlamova, I. S. Lyubutin et al., JETP Lett. 80, 426 (2004)
[3] A. G. Gavriliuk, V. V. Struzhkin, I. S. Lyubutin et al., Phys. Rev. B 71, 155112 (2008)
[4] Y. Ding, D. Haskel, S. G. Ovchinnikov et al., Phys. Rev. Lett. 100, 045508 (2008)
[5] S. Sachdev, Quantum Phase Transitions (Cambridge University Press, Cambridge, 2001)
[6] T. W. B. Kibble, J. Phys. A-Math. Gen. 9, 1387 (1976)
[7] W. H. Zurek, Nature 317, 505 (1985)
[8] W. H. Zurek, Phys. Rep. 276, 177 (1996)
[9] Y. Tanabe, S. Sugano, J. Phys. Soc. Jap. 9, 753 (1954)
[10] S. G. Ovchinnikov, JETP 140, 909 (2008)
[11] L. V. Velikov, A. S. Prokhorov, E. G. Rudashevskii, V. N. Seleznev, JETP 39, 909 (1974)
[12] A. I. Nesterov, S. G. Ovchinnikov, JETPL 90, 580 (2009)
[13] B. Damski, W. H. Zurek, Phys. Rev. A 73, 063405 (2006)
[14] W. H. Zurek, U. Dorner, P. Zoller, Phys. Rev. Lett. 95, 105701 (2005)
[15] B. Damski, Phys. Rev. Lett. 95, 035701 (2005)
[16] M. Abramowitz, I. A. Stegun (Ed.), Handbook of Mathematical Functions (Dover, New York, 1965)
[17] N. N. Lebedev, Special Functions & Their Applications (Dover, New York, 1972)
[18] N. V. Vitanov, B. M. Garraway, Phys. Rev. A 53, 4288 (1966)
[19] N. V. Vitanov, Phys. Rev. A 59, 988 (1999)
[20] S. Suzuki, M. Okada, In: A. Das, B. K. Chakrabarti (Ed.), Quantum Annealing and Related Optimization Methods, Vol. 679 of Lecture Notes in Physics (Springer, 2005) 207
[21] A. Das, B. K. Chakrabarti, Rev. Mod. Phys. 80, 1061 (2008)
[22] J. Roland, N. J. Cerf, Phys. Rev. A 65, 042308 (2002)
[23] L. D. Landau, E. M. Lifshitz, Quantum Mechanics (Pergamon, New York, 1958)
[24] C. Zener, Proc. R. Soc. A 137, 696 (1932)
[25] I. S. Lyubutin, A. G. Gavriliuk, UFN 179, 1047 (2009)